

Continuous-time random-walk model of electron transport in nanocrystalline TiO₂ electrodes

Jenny Nelson

Blackett Laboratory, Imperial College of Science Technology and Medicine, Prince Consort Road, London SW7 2BZ, United Kingdom

(Received 16 November 1998)

Electronic junctions made from porous, nanocrystalline TiO₂ films in contact with an electrolyte are important for applications such as dye-sensitized solar cells. They exhibit anomalous electron transport properties: extremely slow, nonexponential current and charge recombination transients, and intensity-dependent response times. These features are attributed to a high density of intraband-gap trap states. Most available models of the electron transport are based on the diffusion equation and predict transient and intensity-dependent behavior which is not observed. In this paper, a preliminary model of dispersive transport based on the continuous-time random walk is applied to nanocrystalline TiO₂ electrodes. Electrons perform a random walk on a lattice of trap states, each electron moving after a waiting time which is determined by the activation energy of the trap currently occupied. An exponential density of trap states $g(E) \sim e^{\alpha(E_c - E)/kT}$ is used giving rise to a power-law waiting-time distribution, $\psi(t) = At^{-1-\alpha}$. Occupancy of traps is limited to simulate trap filling. The model predicts photocurrents that vary like $t^{-1-\alpha}$ at long time, and charge recombination transients that are approximately stretched exponential in form. Monte Carlo simulations of photocurrent and charge recombination transients reproduce many of the features that have been observed in practice. Using $\alpha = 0.37$, good quantitative agreement is obtained with measurements of charge recombination kinetics in dye-sensitized TiO₂ electrodes under applied bias. The intensity dependence of photocurrent transients can be reproduced. It is also shown that normal diffusive transport, which is represented by $\psi(t) = \lambda e^{-\lambda t}$ fails to explain the observed kinetic behavior. The model is proposed as a starting point for a more refined microscopic treatment in which an experimentally determined density of states can be easily incorporated. [S0163-1829(99)00420-8]

INTRODUCTION

Porous, nanocrystalline semiconducting films of wide band-gap oxides such as TiO₂, WO₃, and ZnO are an important new class of electronic materials. They exhibit extraordinary optical and electronic properties on account of the small grain size and large surface-area-to-volume ratio. When contacted with electrolytic or solid-state hole conductors they form electronic junctions of enormous area. These are useful in applications such as photovoltaics, photocatalysis, and electrochromic, electroluminescent, and bioanalytical devices.¹ Nanocrystalline TiO₂ is of particular relevance for dye-sensitized photovoltaic cells where photovoltaic action occurs at the junction between a porous nanocrystalline TiO₂ film and an electrolyte.^{2,3} The electronic properties of this junction are of interest for optimizing the electrical performance of the photovoltaic device and have been widely studied in that context.

Various observations indicate that electron transport in the nanocrystalline TiO₂ dominates the transient response of the system. Transient photocurrent measurements reveal a very slow (\sim millisecond), multiphasic response to both continuous wave^{4,5} and pulsed^{6,7,8} illumination. The characteristic rise or decay time of the response is dependent upon the intensity of the light source.^{4,7,8,9} Comparison with the transient response without electrolyte indicates that it is the TiO₂, and not the electrolyte, which is responsible for the very long tail.^{10,11} A slow and multiphasic time dependence has also been observed in the rereduction of oxidized dye molecules in a redox inactive environment;¹² the same work indicates that the rate of dye reduction is controlled by the concentration of electrons introduced into the TiO₂ by exter-

nally applied bias. The wide range of time scales is consistent with the assumption that electron transport within the TiO₂ is the rate limiting step.

The slow processes are attributed to the trapping of electrons by a high density of localized states in the TiO₂. Since the TiO₂ grains are normally crystalline,¹³ the localized states are believed to be concentrated at the grain boundaries and on the very large surface. There is evidence for intraband-gap states in bias-dependent optical absorbance spectra¹⁴ and surface photovoltage spectra.¹⁵ It would, therefore, be extremely useful to correlate the density and nature of those states with the electronic transport properties of the material.

A number of models have been applied to current transport in nanocrystalline TiO₂ using conventional semiconductor transport theory. The argument is used that since the crystallites are small (5-25 nm in diameter) and the dopant density in naturally *n*-type TiO₂ is low ($\sim 10^{16} \text{ cm}^{-3}$) (Ref. 16) the electric field, which is established spontaneously within the semiconductor when it comes into contact with the electrolyte, is extremely weak, and the potential is not expected to vary by more than a few meV across a crystallite.¹⁶ If, moreover, the density and mobility of charge carriers in the electrolyte is as high in the nanoporous geometry as it is in the bulk then negligible potential variations are expected across the semiconductor and the electrolyte will maintain the semiconductor surface at a nearly constant potential, so that negligible *macroscopic* electric fields will be permitted across the semiconductor phase. Then electron migration can be neglected and transport can be modeled with the diffusion equation alone. For a system where the carrier density *n* varies only in the *x* direction the electron current

density J_n contains only the diffusion component

$$J_n = qD \frac{\partial n}{\partial x}, \quad (1)$$

where q is the electronic charge and D is the electron diffusion coefficient. Then applying carrier continuity to the electron population we obtain the diffusion equation

$$\frac{\partial n}{\partial t} = D \frac{\partial^2 n}{\partial x^2} + G - R, \quad (2)$$

where G and R represent the volume generation and recombination rate.

The diffusion equation has been applied to nanocrystalline TiO₂ by Sodergren *et al.*¹⁷ and Stangl, Ferber, and Luther¹⁸ to model steady-state electric currents, and by others, e.g., Ref. 6 to model transient currents. The value of D is derived by fitting data. However, diffusion predicts a monoexponential time dependence in the limit of long times, and photocurrent rise and decay times which are independent of intensity, in contradiction with observation. The carrier density dependence that is observed in practice can be reproduced by a modified diffusion equation where the diffusion constant D is made a function of the carrier density n , e.g., Ref. 4. However the physical basis for the choice of $D(n)$ is not clear. Moreover, estimates of the value of D differ by orders of magnitude.¹⁹ It is doubtful whether these approaches can relate observed behavior to materials properties in a useful predictive way.

The role of intraband-gap states in transport within nanocrystalline materials has been recognized by some authors. Schwartzburg and Willig, de Jongh *et al.*, and Dloczik *et al.*^{7,9,20} include terms for trapping and detrapping at a constant rate in the rate equations. This would apply to materials with a dominant trap state at a particular energy within the band gap. Vanmaekelbergh and van Pieterse²¹ present a formulation for the photocurrent that includes thermal activation out of a *distribution* of intraband-gap states, and apply it to nanocrystalline gallium phosphide films. This method could be applied to nanocrystalline TiO₂ if the distribution of trap-state energies were known.

Here we present an alternative approach based on the continuous-time random-walk (CTRW) model of dispersive transport, which includes the distribution of intraband-gap states implicitly. We apply it to the experimental situations of transient photocurrent and charge recombination and in the latter case, show that it is capable of explaining experimental results.

THEORETICAL BACKGROUND

The CTRW was introduced by Scher and Montrol²² (SM) and subsequently developed by other authors²³ in order to explain anomalous slow charge transport in disordered semiconductors such as As₂Se₃. Time of flight measurements indicated a power-law dependence of the induced current, at variance with conventional theory. In the CTRW, charge carriers execute a random walk independently on a lattice, taking each step after an interval which is drawn from a waiting-time distribution (WTD) $\psi(t)$. This distribution of waiting times can represent the disorder in either activation

energies (energetic disorder) or carrier locations (configurational disorder) or both.²⁴ Energetic disorder is important for systems where carriers move predominantly by thermal activation out of and capture into trap states. Configurational disorder is most important when carrier move by tunnelling, or hopping, between localized states. The form of $\psi(t)$ is determined by the dispersion in those quantities: for the case of activation out of trap states $\psi(t)$ is directly related to the density of states $g(E)$ of the traps. It is straightforward to show that an exponential distribution of activation energies $g(E) \sim e^{-E_{act}/kT_0}$, as would be expected for an Urbach tail in the conduction-band edge, leads to the power-law form for $\psi(t)$

$$\psi(t) = A t^{-1-\alpha}, \quad (3)$$

where $0 < \alpha < 1$ and

$$\alpha = \frac{T}{T_0}. \quad (4)$$

The exponent α is a measure of the degree of disorder. A small α implies a long tail in the intraband-gap distribution of states, and hence a highly disordered medium.

It has been shown that a power-law WTD can arise from either trapping/detrapping, hopping, or thermally assisted hopping between states which possess an exponential energy distribution.²⁵ Therefore, the WTD alone does not specify uniquely the mechanism of carrier transport.

With a power-law $\psi(t)$ the model predicts a power-law behavior for the photocurrent transient $I(t)$ such that $I(t) \sim t^{-1+\alpha}$ at short times $I(t) \sim t^{-1-\alpha}$ at long times. In their original model SM include an asymmetry in the stepping probability to represent the electric field in a biased photoconductor. They need to consider only one carrier type to simulate the time of flight experiments since the initial sheet of charge is narrow and only one carrier type is capable of moving away from the illuminated surface, when the sample is biased. More recently similar models have been applied to explain dispersive transport in semiconducting polymers^{26,27} and metal oxides.²⁸

Variants have been developed to model charge recombination inside disordered materials (the ‘‘target annihilation’’ model)²⁹ and charge trapping.³⁰ In the target annihilation model the survival probability S of an immobile species which reacts with the walking electron is expected to vary like a stretched exponential at long times, $S(t) \sim e^{-\lambda t^\alpha}$, where λ is proportional to the number of walkers, provided that walkers greatly outnumber targets.

The CTRW includes ‘‘normal’’ diffusion as the special case where $\psi(t) = (1/\tau)e^{-t/\tau}$. Here, the Poisson distribution follows from a unique ‘‘activation’’ energy as would be expected for a uniform conduction band. The diffusion constant is then related to the mean step time τ and the step length L through $D = L^2/6\tau$. The CTRW with Poisson distribution $\psi(t) = 1/\tau e^{-t/\tau}$ is also statistically identical to the simple RW of time step τ .

MODEL

In this paper, we apply the CTRW to nanocrystalline TiO₂ in order to simulate the two experimental simulations, (a)

transient photocurrent in response to a cw illumination and (b) the rereduction of oxidized dye molecules by mobile electrons (here called *charge recombination*) as studied by Haque *et al.*¹² We are encouraged to use this model by the observations that (i) current transients drawn from TiO₂ electrodes are nonexponential at long times, varying algebraically with time in at least one case¹¹ and (ii) charge recombination rates are approximately stretched exponential in form.

Choosing the CTRW involves making a number of assumptions. First, electric fields are neglected. For nanocrystalline TiO₂ this is justified above. Second, only one carrier type is involved in transport. This is likely to be true for the case where electrons are generated by excitation of a dye, rather than by band-gap excitation, since no mobile holes are created. Clearly the motion of charge carriers in the electrolyte through the pores of the semiconductor is an important feature of the nanocrystalline junction, but it is not included in this model. Rather, the electrolyte is considered as an effective medium that screens out Coulombic forces and allows the electrons to move within the semiconductor in a truly Brownian manner. Third, motion of *untrapped* carriers is neglected. This is supported by estimates that the population of trapped carriers greatly outnumbers the untrapped.⁹ And by the very much longer times for release from deep traps than for thermal hopping within the conduction band. In fact, the diffusion of carriers between trapping events can be included within an *effective* WTD, and so the model can be extended in this way. For nanocrystalline films where trap states are most likely situated on the surface the specific film morphology is likely to be important. This is the subject of a separate study.³¹

In our application of the CTRW we make the further assumptions that charge recombination with defects and the electrolyte, can be neglected, and that the energetic distribution of electron trap states $g(E)$ is exponential below the conduction band. Recombination with holes, iodide, or impurities would be straightforward to include if appropriate values for the recombination lifetime were known. A different $g(E)$ would be equally easy to include.

Finally, in applying a current transport model to the dynamics of reduction of dye cations we have made an assumption that electron transport in the TiO₂ is the rate limiting step in this process. It is not at all obvious that this should be the case, however the results presented below are plausible enough to indicate that it *could* be. A detailed assessment of other possible mechanisms controlling this reaction is in progress.

The nanocrystalline film is modeled as a regular, cubic lattice where each site possesses a trap energy E drawn from the distribution

$$g(E) = \frac{1}{kT_0} e^{E/kT_0}, \quad E < E_c. \quad (5)$$

If carriers leave the site by thermal activation through $E_{\text{act}} = E_c - E$, the release or waiting time is given by

$$t = \tau_{th} e^{-E/kT}, \quad (6)$$

where τ_{th} is a minimum thermal activation time, determined by the thermal frequency of the semiconductor, and the

conduction-band edge energy E_c is set to 0. Equations (5) and (6) are equivalent to drawing a time t from the distribution

$$t = \tau_{th} [\text{Rnd}(0,1)]^{-1/\alpha}, \quad t \geq \tau_{th},$$

where $\text{Rnd}(0,1)$ is a random number between 0 and 1. This delivers the power law WTD, Eq. (3), with prefactor

$$A = \alpha \tau_{th}^\alpha. \quad (7)$$

At the start of the simulation n_i carriers per unit volume are located at random on lattice sites. n_i is the sum of the dark electron density n_d and a photogenerated electron density n_g . The dark carriers are located completely at random, while for the photogenerated carriers the x coordinate is chosen from the distribution

$$\frac{e^{-\alpha x}}{(1 - e^{-\alpha d})},$$

where σ is the optical absorption coefficient and d is the film thickness. Each carrier adopts the waiting time of its host site. The carrier with the shortest time t_1 moves in a random direction to a neighboring site and adopts the waiting time of that site while the release times of the other carriers are advanced by t_1 .

In case (a) optical generation is dominant and n_d is neglected. For cw illumination one new photogenerated carrier is introduced every $1/g_0$ seconds, where g_0 is the optical generation rate. For illumination by a pulse of light, n_g carriers are introduced at $t=0$. We apply the boundary conditions that no carriers pass through the boundary at $x=0$, (i.e., a blocking contact, which represents the TiO₂-electrolyte interface) while all carriers that reach the Ohmic contact at $x=d$ (TiO₂-conducting glass interface) are collected. The same boundary conditions are applied by Cao *et al.*⁴ to the same problem. This is consistent with experimental evidence^{8,15} for a space charge layer at the SnO₂:TiO₂ interface, which aids electron collection. Periodic boundary conditions are applied in the y and z directions. Carriers reaching the collecting boundary are recorded and constitute the photocurrent.

In case (b), we have

$$n_i = n_d(E_F) + S_0, \quad (8)$$

where

$$n_d(E_F) = \int_{-\infty}^{\infty} g(E) \frac{1}{e^{(E-E_F)/kT} + 1} dE, \quad (9)$$

where E_F is the electron quasi-Fermi level in the film. For the exponential distribution of trap states (5), with $T_0 > T$ this approximates to

$$n_d = n_{d0} e^{\Delta E_F / kT_0}, \quad (10)$$

where n_{d0} is the density of electrons in the dark at zero bias, and ΔE_F is the increase in E_F due to the applied bias. In an ideal system ΔE_F should be equal to the applied bias V . S_0 is the density of optically excited dye molecules, each of which is assumed to contribute one electron to the semiconductor. In addition, S_0 static target sites are created, repre-

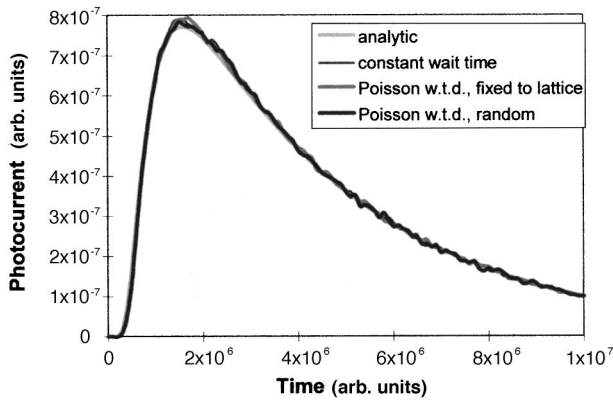


FIG. 1. Test simulations of photocurrent transient in response to a pulse of light for normal diffusion. The curves represent simulations of a normal random walk with constant time step $\tau = L^2/6D$; a CTRW with waiting times drawn at random from the distribution $(1/\tau)e^{-t/\tau}$; and a CTRW where the waiting times are drawn from the same distribution but are associated with lattice sites. All agree with the analytic solution of the diffusion equation, with diffusion coefficient $D = L^2/6\tau$, where L is the RW step length, also shown.

senting the oxidized dye molecules with which the mobile electrons may recombine. In this case, periodic boundary conditions are applied in all directions. This supposes that the optical depth of the film is small and that the collected current over the time taken to reduce all oxidized dyes is negligible. In these conditions the film is statistically homogenous and the continuity equation [Eq. (2)] reduces to a time-dependent problem. During the simulation, when a carrier moves into a site occupied by a target and both are annihilated. The simulation finishes when all targets are exhausted.

As a test of the CTRW we apply it to cases (a) and (b) with a Poisson waiting-time distribution, representing normal diffusion. In these cases the diffusion equation can be solved analytically. We obtain identical results to the diffusion equation for the cases when the waiting time is drawn at random from the distribution for each step, and when the wait time is associated with the lattice site.

Figure 1 shows the results of test simulations of a time-of-flight photocurrent transient. Notice how the three versions produce identical results, and agree with the analytic solution. Similar agreement is obtained for the different versions in the other cases.

We make one further modification to the SM model: as a simulation of the trap filling effect we allow lattice sites to be occupied by only one electron. This means that as carrier density increases the deeper states are likely to be full, and so mobile carriers are more likely to occupy shallow traps and so are more likely to move, on the whole, more quickly. This is what is observed in practice. The trap-filling effect is less relevant for the time-of-flight measurements modeled by SM since they were concerned with reverse bias conditions where carrier densities are low.

It may be useful to compare our model with previous Monte Carlo simulations of the CTRW reported in Refs. 25 and 26. In common with those simulations, our simulation is carried out on a regular cubic lattice with each carrier moving to one of a number of neighboring sites after a waiting time associated with its position. Original Monte Carlo simu-

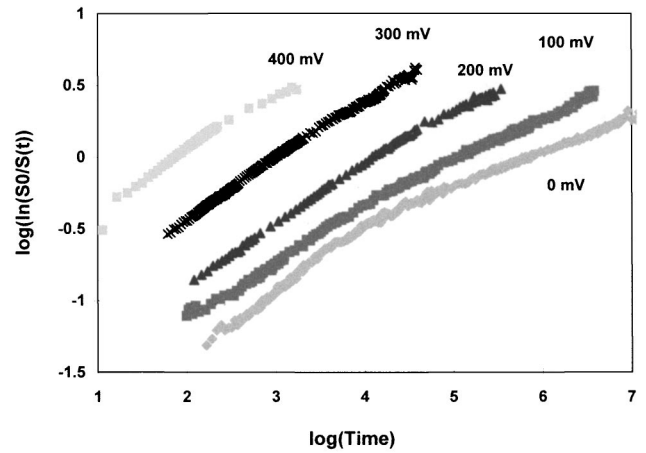


FIG. 2. Charge recombination data from Ref. 12 replotted in a form that shows that the form of the oxidized dye density $S(t)$ is approximately stretched exponential with $\alpha = 0.39 \pm 0.4$. The survival probability $S(t)/S_0$ is obtained by dividing the change in optical density, as reported in Ref. 12, by its initial value.

lations of dispersive transport²⁵ used a WTD governed either by the difference in energies of the original and destination sites (to represent thermally assisted hopping) or by the original site energy alone (to represent thermal activation out of traps). Since the kinetics resulting from these were indistinguishable we choose to use the latter model as it is slightly easier to compute. Also for reasons of computer time we include carrier transfer only to nearest-neighbor sites rather than to several orders of nearest neighbors. In contrast to those simulations, we do not include a bias in our modeling of the transient photocurrent since this is not appropriate for the experimental data we consider. We do, however, introduce a rule to prevent multiple occupancy of sites, in order to simulate trap filling as explained above. Our modeling of charge recombination in case (b) is comparable with the numerical simulation of target annihilation reported in Ref. 24, when that is extended to three dimensions.

RESULTS

Choice of parameters

For both types of simulation we need the two parameters τ_{th} and α , which determine the WTD. For τ_{th} we have used a value of 5×10^{-15} s, which gives good agreement with the experiment in case (b), and compares fairly well with the thermal hopping time of 1.5×10^{-15} s derived from the published diffusion constant and activation energy for electrons in rutile TiO_2 .³² We estimate α by ‘‘stretched exponential’’ analysis of the charge recombination data of Haque *et al.* By fitting a function of the form

$$S(t) = S_0 e^{-\lambda t^\alpha} \quad (11)$$

to the data we obtain values of α in the range $0.35 < \alpha < 0.43$ for applied biases in the range 0 to 0.5 V (Fig. 2). We use $\alpha = 0.37$ in the simulations below.

The density of trap states N_t is needed in both cases. In case (a), N_t depends on the lattice constant L through $N_t = L^{-3}$, while in case (b) it is the ratio of traps to targets that matters. The density of trap sites on the *surface* of nanocryst-

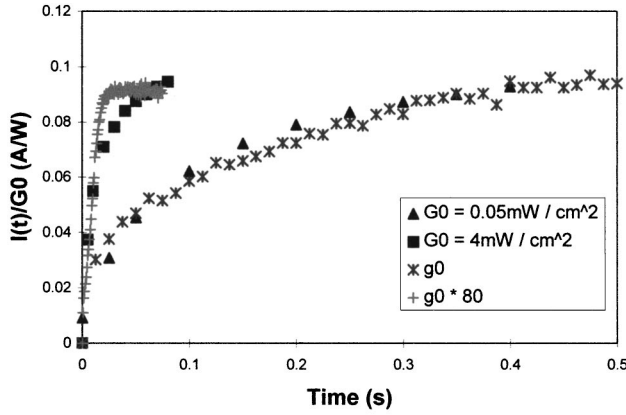


FIG. 3. Simulated photocurrent transients in response to *cw* illumination, in comparison with photocurrent data taken from Ref. 4. The ratio of photocurrent to intensity is plotted in order to emphasize the effect of state filling on the transients. For the simulation, $\alpha=0.37$ and values of the minimum release time τ_{th} and generation rate g_0 are taken to produce a curve (*), which matches the low-intensity data. The high-intensity curve (+) was obtained by increasing g_0 by a factor of 80.

talline TiO_2 is quoted as of the order of 10^{17} m^{-2} ,¹⁶ which means several hundred traps in a nanoparticle of 10 nm radius.

Case (a) Simulation of photocurrent transients

With the present model it is prohibitively slow to simulate the CTRW through a film containing realistic numbers of traps. For instance, with 500 traps per nanoparticle we would need a lattice several thousand units wide to represent an 8- μm thick film. To improve speed of simulation we renormalize the lattice into a “superlattice” where each trapping event at a superlattice site represents the net delay due to trapping in a *group* of sites. It can be shown by examining the WTD’s in the Laplace domain that a power-law WTD gives rise to a WTD for the group of sites of size $N \times N \times N$, which also varies like $t^{-1-\alpha}$ at long times, but is reduced in magnitude by a factor N . For the simulations reported here we use a superlattice 40 units wide. This is roughly equivalent to $N=50$ to 70, for a trap density of 100–500 per particle. Below we present exemplary results that demonstrate qualitative features. Quantitative compar-

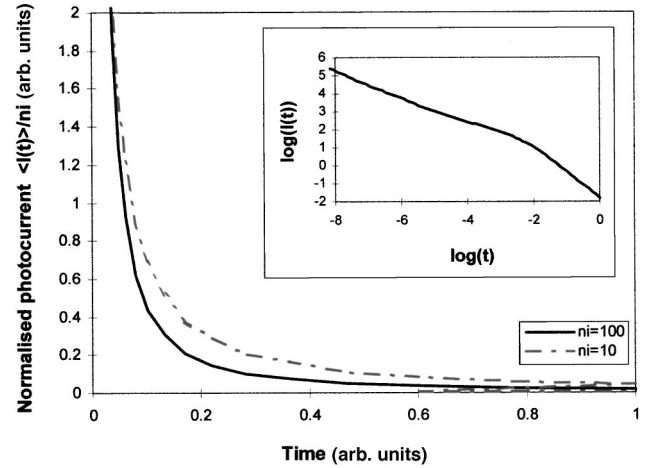


FIG. 4. Simulated photocurrent transient in response to an initial pulse of light, with $\alpha=0.37$, and photogenerated electron densities of 10 (dashed line) and 100 (full line) electrons per 64 000 trap states. Notice how the normalized photocurrent decays more quickly as n_i is increased. The inset shows the power law form of the photocurrent $I(t)$ varying like $t^{-1+\alpha}$ at short time and $t^{-1-\alpha}$ at long time.

son with data is not possible since we do not presently have access to data for which all relevant parameters are known.

For *cw* illumination, the simulations resemble the observed intensity dependence. Figure 3 shows the simulated normalized photocurrent $I(t)/g_0$ in comparison with measured intensity dependent data from Ref. 4, replotted as a fraction of intensity. Plotting this quantity emphasises the effect of trap filling since $I(t)/g_0$ should have a universal form if trap occupancy has no effect on the motion. For this comparison τ_{th} and g_0 were chosen to fit the low-intensity transient from Ref. 4, and the simulation repeated with g_0 increased by a factor of 80 to simulate the higher intensity transient. The value of τ_{th} was 5×10^{-13} s longer than the thermal hopping frequency discussed above. This disagreement may be in part due to the neglect of recombination with the electrolyte in the present model, or to the distortion of the short-time behavior of the WTD after renormalization. A more quantitative comparison is not possible without knowing the optical depth of the films and the quantum efficiency for current collection. Nevertheless, the encouraging agreement shows that the CTRW model has the capability of modeling photocurrent transients.

TABLE I. Values of the initial dark electron density n_{0d} as a fraction of initial oxidized dye density S_0 for different values of the electron quasi Fermi level ΔE_F , used in simulations of charge recombination. In the left-hand set of columns series resistance is neglected and it is assumed that the shift in Fermi level is equal to q times the applied bias. The values on the right are calculated using a series resistance of 5000 Ω , estimated from measurements of the dark current (Ref. 33).

Applied bias (mV)	Neglecting series resistance		Including series resistance	
	ΔE_F (meV)	n_{0d}/S_0	ΔE_F (meV)	n_{0d}/S_0
0	0	0.1	0	0.1
100	100	0.4	90	0.4
200	200	1.8	190	1.8
300	300	7.4	280	5.5
400	400	31.0	370	20.1
500	500	130.1	430	47.7

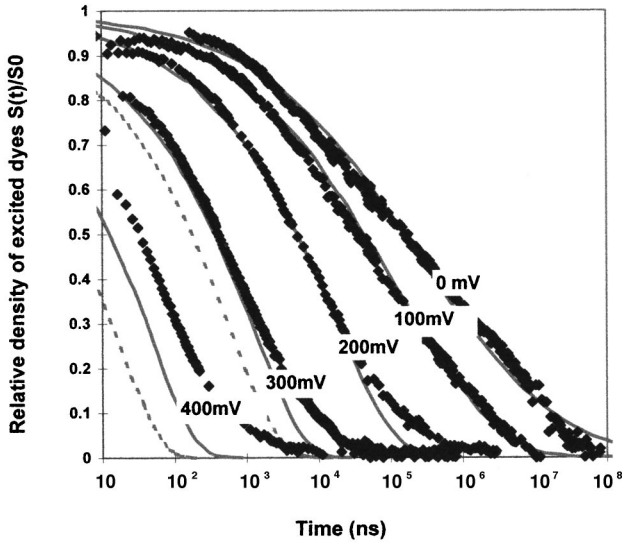


FIG. 5. Simulated dye survival probability $S(t)/S_0$ at various applied biases in comparison with charge recombination data from Ref. 12, replotted as the change in optical depth relative to its initial value (full diamonds). Simulations were made with $\alpha=0.37$, minimum release time $\tau_{th}=5\times 10^{-15}$ s and initial dark electron densities as given in Table I. The full gray lines were obtained when the electron Fermi level was adjusted for series resistance. The dashed gray lines show the simulation results for biases $V=300$ and 400 mV when series resistance is neglected.

Simulated time-of-flight experiments reproduce the power-law transient behavior of $I(t)$ reported by SM. When trap filling is included in the model the characteristic decay time is dependent on the intensity of the original pulse, while the power-law form at long t is the same. These effects are illustrated in Fig. 4 showing simulation results for $I(t)/n_i$ at two different n_i , representing two different pulse intensities.

Case (b) Simulation of charge recombination

In this case, the spatial resolution has no effect and N_t appears through the *relative* population of trap states and target sites, N_t/S_0 . Since Haque *et al.* excite approximately one dye per nanoparticle N_t should outnumber S_0 by several hundred. In the simulations below we use $N_t/S_0=640$. Provided that it is large, changing this ratio primarily affects the time scale and so N_t is not independent of τ_{th} .

The initial electron population in the dark is estimated from the natural doping density of nanocrystalline TiO_2 . Using $N_d=10^{22}\text{ m}^{-3}$ (Ref. 16) we expect an average electron density in the dark n_{d0} of around 0.1 per 10 nm radius nanoparticle in an unbiased film. With an increase in applied bias of δV this density is increased by the factor $e^{q\delta V/kT}$, from Eq. (10) using the exponential distribution of trap states (5) and assuming that a shift in bias translates entirely into a shift in electron Fermi level. The relative densities of electrons and targets as a function of shift in Fermi level are given in Table I. To avoid dealing with fractional n_i we set S_0 to a multiple of 10 so that the lattice represents several nanoparticles, which share the dark electrons.

Results of simulations are presented in Fig. 5. The model reproduces the shape of the transients fairly well, and predicts the change in shape as the electron density overtakes

the target density. The model underestimates the survival probability $S(t)$ at high forward biases if it is assumed that all of the change in electrostatic bias translates into a change in electron Fermi level, i.e., $\Delta E_{Ff}=qV$. However if part of the bias is dropped through series resistance in the conducting glass and electrolyte or elsewhere in the system then $\Delta E_F < qV$ and agreement improves. In fact there is preliminary experimental evidence which indicates that at these biases there is a small dark current and a series resistance of around $5000\ \Omega$.³³ When this is taken into account the effective bias is reduced as shown in Table I and good quantitative agreement is obtained for biases up to 300 mV. At low biases where $n_i \rightarrow S_0$ the model predicts a decreasing sensitivity to bias and the $S(t)$ converge on a universal curve. This is observed experimentally.³⁴

To compare model and data at high forward bias we may consider the bias dependence of the half time $t_{50\%}$, defined such that $S(t_{50\%}) = \frac{1}{2}S_0$. By a straightforward theoretical argument using Eqs. (10) and (11) the model predicts $t_{50\%} \propto e^{-q\delta V/kT}$ at high biases, in contrast with the experimental result, $t_{50\%} \propto e^{-q\delta V/(1.7 \pm 0.25)kT}$. The different limiting forms suggest that $\Delta E_F < V$ at high V . There are a number of possible explanations. One is that the Coulombic exchange energy experienced by electrons inside the nanoparticles is significant. Another is that a second recombination avenue competes for the electrons with the oxidized dyes, constituting a dark current.

Alternatively, the different limiting behavior could be due to oversimplifications in the model. For example, the model assumes a homogenous distribution of trap states while in reality traps are likely to be concentrated on two-dimensional (2D) surfaces embedded within the 3D medium. Another possibility is that rereduction of the oxidized dye is not diffusion limited, i.e., the probability does not depend directly on the product of electron and oxidized dye densities but more weakly on the electron density. In RW terms that means the electron visits the oxidized dye several times before reducing it. All of these issues are being addressed in a more detailed model currently under development.³¹

Disagreement in the *shape* of the transients is likely to be related to the shape of the density of trap states. The exponential form was assumed here in the absence of any better information. Once a more realistic $g(E)$ is available, it will be easy to incorporate.

CONCLUSION

Conventional semiconductor transport theory based on the diffusion equation fails to explain the observed asymptotic behavior and intensity dependence of current transport in nanocrystalline TiO_2 electrodes. A model of dispersive transport using a continuous-time random walk, where the waiting times for electron motion are directly related to the energetic distribution of trap states, explains several features. Notably, the asymptotic time behavior is roughly consistent with an exponential energy distribution of trap state energies; the intensity dependence of photocurrent transients can be explained by trap filling; and shape and bias dependence of charge recombination kinetics are partly explained. At large forward biases the model overestimates the charge recombination rate and it is not clear whether this is due to uncer-

tainties in the experimental conditions or oversimplifications in the model.

The model offers the possibility of relating the form of transient features to the density of trap states. Further issues remain to be resolved before we can fully develop a microscopic model. For instance, we need to establish whether transport is dominated by hopping or thermal activation and understand how properties are changed by the presence of a contacting layer at the surface. These can be resolved by a series of systematic time, intensity, and temperature-dependent measurements of nanocrystalline TiO₂ films. We also need to examine other possible mechanisms causing a

wide range of time scales for charge recombination. All of these are the subject of future studies.

ACKNOWLEDGMENTS

This work was supported by the Engineering and Physical Sciences Research Council and the Greenpeace Environmental Trust. I am grateful to Saif Haque for the communication of dark current measurements prior to publication and for permission to use data from Ref. 12 in the form presented here. I would also like to thank James Durrant and Jeff Miller for many helpful consultations.

- ¹See, e.g., J. M. Stipkala, F. N. Castellano, T. A. Heimer, C. A. Kelly, K. J. T. Livi, and G. J. Meyer, *Chem. Mater.* **9**, 2341 (1997).
- ²B. O'Regan and M. Grätzel, *Nature (London)* **353**, 737 (1991).
- ³A. Hagfeldt and M. Grätzel, *Chem. Rev.* **95**, 49 (1995).
- ⁴F. Cao, G. Oskam, G. J. Meyer, and P. C. Searson, *J. Phys. Chem.* **100**, 17 021 (1996).
- ⁵P. M. Sommeling, H. C. Rieffe, J. M. Kroon, J. A. M. van Roosmalen, A. Schonecker, and W. C. Sinke, in *Proceedings of the 14th EC Photovoltaic Solar Energy Conference*, edited by H. Ossenbrink, P. Helm, and H. Ehmman, (H.S. Stephens and Associates, Bedford, 1997), pp. 1816–1819.
- ⁶A. Solbrand, H. Lindstrom, H. Rensmo, A. Hagfeldt, S.-E. Lindquist, and S. Sodergren, *J. Phys. Chem. B* **101**, 2514 (1997).
- ⁷K. Schwarzburg and F. Willig, *Appl. Phys. Lett.* **58**, 2520 (1991).
- ⁸B. Levy, W. Liu, and S. E. Gilbert, *J. Phys. Chem. B* **101**, 1810 (1997).
- ⁹L. Dloczik, O. Ieperuma, I. Lauer mann, L. M. Peter, E. A. Ponomarev, G. Redmond, N. J. Shaw, and I. Uhlendorf, *J. Phys. Chem. B* **101**, 10 281 (1997).
- ¹⁰A. Hagfeldt, S.-E. Lindquist, and M. Grätzel, *Sol. Energy Mater. Sol. Cells* **32**, 245 (1994).
- ¹¹R. Konenkamp, R. Henninger, and P. Hoyer, *J. Phys. Chem.* **97**, 7328 (1993).
- ¹²S. A. Haque, Y. Tachibana, D. R. Klug, and J. R. Durrant, *J. Phys. Chem. B* **102**, 1745 (1998).
- ¹³C. J. Barbe, F. Arendse, P. Compte, M. Jirousek, F. Lenzmann, V. Shklover, and M. Grätzel, *J. Am. Ceram. Soc.* **80**, 3157 (1997); also, Raman spectroscopy of nanophase TiO₂ produced by three different methods indicates clearly that the material takes the anatase crystalline form in all cases [N. Malde and J. Nelson (unpublished)].
- ¹⁴F. Cao, G. Oskam, P. C. Searson, J. M. Stipkala, T. A. Heimer, F. Farzad, and G. J. Meyer, *J. Phys. Chem.* **99**, 11 974 (1995).
- ¹⁵E. Moons and M. Grätzel (unpublished)
- ¹⁶G. Rothenberger, D. Fitzmaurice, and M. Grätzel, *J. Phys. Chem.* **96**, 5983 (1992).
- ¹⁷S. Sodergren, A. Hagfeldt, J. Olsson, and S.-E. Lindquist, *J. Phys. Chem.* **98**, 5552 (1994).
- ¹⁸R. Stangl, J. Ferber, and J. Luther, *Proceedings of the 14th EC Photovoltaic Solar Energy Conference* (Ref. 5), pp. 2526–2529.
- ¹⁹Reference 18 finds $D=8\times 10^{-7}\text{ m}^2\text{ s}^{-1}$; Ref. 10 finds D in the region of $5\times 10^{-9}\text{ m}^2\text{ s}^{-1}$; Ref. 9 finds $1.5\times 10^{-9}\text{ m}^2\text{ s}^{-1}$, all in contrast with the value for bulk (rutile) TiO₂ of $1.5\times 10^{-6}\text{ m}^2\text{ s}^{-1}$ (Ref. 35).
- ²⁰P. E. de Jongh and D. Vanmaekelbergh, *J. Phys. Chem. B* **101**, 2716 (1997).
- ²¹D. Vanmaekelbergh and L. van Pieter son, *Phys. Rev. Lett.* **80**, 821 (1998).
- ²²H. Scher and E. W. Montroll, *Phys. Rev. B* **12**, 2455 (1975).
- ²³See, e.g., M. Silver and L. Cohen, *Phys. Rev. B* **15**, 3276 (1977); T. Tiedje and A. Rose, *Solid State Commun.* **37**, 49 (1980); F. W. Schmidlin, *Phys. Rev. B* **16**, 2362 (1977); F. B. McLean and G. A. Ausman, *ibid.* **15**, 1052 (1977).
- ²⁴J. Ross MacDonald, *Impedance Spectroscopy* (Wiley, New York, 1980).
- ²⁵M. Silver, G. Schönherr, and H. Bässler, *Phys. Rev. Lett.* **48**, 352 (1982); M. Silver and L. Cohen, *Phys. Rev. B* **15**, 3276 (1977).
- ²⁶H. Bässler, *Phys. Status Solidi B* **175**, 15 (1993).
- ²⁷P. W. M. Blom and M. C. J. M. Visenberg, *Phys. Rev. Lett.* **80**, 3819 (1998).
- ²⁸S. Lathi and A. Das, *J. Appl. Phys.* **77**, 3864 (1995).
- ²⁹A. Blumen, G. Zumofen, and J. Klafter, *Phys. Rev. B* **30**, 5379 (1984).
- ³⁰A. Blumen and G. Zumofen, *J. Chem. Phys.* **77**, 5127 (1982).
- ³¹J. B. Miller, M.Sc. thesis, Imperial College of Science Technology and Medicine, 1998.
- ³²The definition of the diffusion constant $D=a_0^2\nu\exp(-\Delta G/kT)$ can be used to calculate the thermal hopping frequency $\nu=6.6\times 10^{14}\text{ s}^{-1}$ from the hopping activation energy (Ref. 35) $\Delta G=0.06\text{ eV}$, the diffusion constant (Ref. 35) $D=1.55\times 10^{-6}\text{ m}^2/\text{s}$, and the lattice parameter $a_0=1.6\text{ \AA}$.
- ³³S. A. Haque (private communication).
- ³⁴S. A. Haque, Y. Tachibana, R. L. Willis, J. E. Moser, M. Grätzel, D. R. Klug, and J. R. Durrant (unpublished).
- ³⁵B. Poumellec, J. F. Marucco, and F. Lagnel, *Phys. Status Solidi A* **89**, 375 (1985).